PAPER NAME

Interdecadal variation of tropical cyclone genesis longitudes over the western North Pacific

AUTHOR

-

WORD COUNT

6469 Words

CHARACTER COUNT

31696 Characters

PAGE COUNT

31 Pages

FILE SIZE

6.4MB

SUBMISSION DATE

Feb 23, 2023 5:00 PM GMT+8

REPORT DATE

Feb 23, 2023 5:01 PM GMT+8

44% Overall Similarity

The combined total of all matches, including overlapping sources, for each database.

- 35% Internet database
- 44% Publications database
- Crossref database
- Crossref Posted Content database
- 0% Submitted Works database

Excluded from Similarity Report

- Bibliographic material

Interdecadal variation of tropical cyclone genesis longitudes over the western North Pacific

JaeWon Choi[1,3] and Kyong-Hwan Seo [1,2,3*]

[1]BK21 School of Earth and Environmental Systems, Pusan National University, Busan, Republic of Korea

[2]Department of Atmospheric Sciences, Pusan National University, Busan, Republic of Korea

[3]Research Center for Climate Sciences, Pusan National University, Busan, Republic of Korea

*Corresponding author: Kyong-Hwan Seo, Professor
Department of Atmospheric Sciences,
Pusan National University,
Geumjeong-gu, Busan, 46241, Republic of Korea
E-mail: khseo@pusan.ac.kr

Abstract

The genesis longitudes of the tropical cyclone (TC) for the months of June–October exhibit the gradual westward shift since 1998 and the present study investigates the possible mechanisms. The period of 1998-2020 is characterized by the large anomalous anticyclonic circulation over the western North Pacific (WNP) and an anomalous cyclonic circulation in East Asia. Owing to this huge anomalous anticyclonic circulation, TCs could not develop over the eastern part of the WNP. In addition, the equatorial western Pacific shows a warm anomaly, while the equatorial eastern Pacific presents a cold anomaly; this negative phase of the Pacific Decadal Oscillation (PDO) demonstrates the strengthening of the Walker circulation, which causes greater prevalence of TCs to the western seas of the WNP.

Key words: western North Pacific, tropical cyclone, Pacific Decadal Oscillation, Walker circulation

1. Introduction

The western North Pacific (WNP) is the water body where tropical cyclone (TC) activity is the most active on Earth. The TCs that occur in these waters migrate west to affect southern China or Vietnam or north to affect the mid-latitude region of East Asia. The regions affected by TCs are mostly determined by the location of TC genesis (Chia and Ropelewski, 2002; Wang and Chan, 2002). The TCs that occurred in the southeastern waters of the WNP migrate northwest and recurve in the East China Sea and eventually affect East Asia. As these TCs travel long distances over the ocean, they gain sufficient energy from the ocean to generate higher intensity and affect the mid-latitude region of East Asia. Meanwhile, TCs that occur in the northwestern waters of the WNP generally migrate short distances to the west to affect southern China and Vietnam. These TCs generally have low intensity because of the topographical effect of the Philippines.

Studies have focused on the tendency of TCs to occur over the western part of the WNP and have revealed that the tropical upper-tropospheric trough (TUTT), monsoon trough, and El Niño-Southern Oscillation (ENSO) affected WNP TC genesis locations (Huang et al. 2016; Wang and Wu 2016; Huangfu et al. 2017; Deng. et al. 2018). Wu (2015) argued that the westward shift of the TUTT is responsible for the westward movement of the WNP TC genesis location, while Huang et al. (2017) attributed this to the recent westward migration of the monsoon trough. Hu et al. (2018) recently reported that more TCs tended to occur in the northwestern part of the WNP and showed that this was related to a shift in convective anomalies for El Niño-Southern Oscillation (ENSO) and a climate regime shift in the Pacific Ocean in 1998. Through observational data analysis and model simulations, Cao et al. (2019) suggested that changes to the La Niña-type Pacific sea surface temperature (SST), which induced the recent global warming hiatus, are responsible for the northwest migration of the location of the WNP TC genesis.

Many studies have shown that the WNP TC genesis is affected by ENSO on the interannual timescale (Lander 1994; Chan 2000; Wang and Chan 2002; Camargo and Sobel 2005; Camargo et al. 2007; Zhao et al. 2010; Kim et al. 2011; Wang et al. 2013; Wang and Wu 2016). ENSO is the large-scale SST fluctuation that occurs in the tropical WNP and the resultant changes in air–ocean circulation affect TC genesis in various regions. Gray (1984) showed that ENSO affected hurricane genesis in the North Atlantic region and Hastings (1990) found that the frequency of tropical disturbances in the southwestern Pacific increased in the eastern region of Australia during anti-El Niño years. Chia and Ropelewski (2002) and Wang and Chan (2002) showed that El Niño years have a strong tendency for WNP TCs to occur in the southeastern waters of the WNP, whereas in La Niña years, they clearly occur in the northwestern part of the WNP. It is also well known that ENSO affects the TC tracks (Kim and Seo 2016).

It is well known that SST is an important environmental factor influencing TC activity. In a study on the relationship between Pacific Decadal Oscillation (PDO) and TC, Lee et al. (2021) indicated that the frequency of TCs passing through Korea and Japan during the negative phase of PDO increased by approximately 50%, compared to those in the positive phase. Wang and Liu (2016) investigated how PDO modulates the effect of ENSO on the rapid intensification (RI) of TCs in the WNP. The relationship between ENSO and RI frequency was shown to be statistically significant in the warm PDO phase. Scoccimarro et al. (2021) showed that PDO modulates TC days in the North Pacific Ocean. In addition, many other studies have investigated the association between TC activity and PDO (Zhou et al. 2007; Kubota and Chan

2009; Liu and Chan 2008, 2013; Yang et al. 2018). So far, however, no studies have been conducted that the westward shift of the WNP TC genesis location during peak TC season (June to October) is associated with PDO. Therefore, we analyze the relationships between the westward shift of the WNP TC genesis location during peak TC season and the PDO on a decadal timescale.

In Section 2, the data and analysis methods are introduced, and in Section 3, a time series of TC genesis longitude locations is analyzed. In Section 4, the recent westward shift of the WNP TC genesis location and atmospheric circulations is analyzed. In Section 5, the effect of SST variation on the recent westward shift of the WNP TC genesis location is analyzed. The results of this study are summarized in Section 6.

2. Data and methodology

2.1 Data

The best-track data produced by the Regional Specialized Meteorological Center–Tokyo Typhoon Center were used as the TC data. These data provide information such as latitude, longitude, central pressure, and maximum sustained wind speed of TCs that have occurred in the WNP since 1951 at six-hour intervals. To analyze large-scale environment and atmospheric circulation regarding the cause of TC activity change, Reanalysis-2 (R-2) monthly average data distributed by the National Center for Environmental Prediction–Department of Energy were used (Kanamitsu 2002). These data consist of 2.5° × 2.5° latitude–longitude grid spacing with a total of 17 vertical layers from 1979 to 2020. Extended Reconstructed Sea Surface Temperature (ERSST) V3b (Smith et al., 2008) data were used as the SST data. ERSST data are the monthly averages from 1854 to the present and consist of 2° × 2° grid spacing. Outgoing longwave radiation (OLR) data were also analyzed (Liebmann and Smith, 1996). In this study, the PDO index (Mantua et al., 1997) was obtained from the website of the University of Washington (http://jisao.washington.edu/pdo).

2.2 Methodology

The vertical wind shear (VWS) for diagnosing large-scale conditions was calculated as follows:

$$VWS = \sqrt{(u_{200-850})^2 + (v_{200-850})^2} \cdot$$

Here, u and v indicate the zonal and meridional flows, respectively. The numbers 200 and 850 represent the 200-hPa and 850-hPa levels, respectively (Wingo and Cecil 2010). The genesis potential index (GPI) was calculated according to the equation of Camargo et al. (2007). A two-tailed Student's t test was used to determine the significance of the results (Wilks 1995).

3. Time series analysis

Figure 1 shows the time series of TC genesis longitude averaged during June–October for 1979–2020 (red line with dots). This time series has distinct interannual and interdecadal variations. The time series shows a decreasing trend until recently (significant at the 90% confidence level), indicating a strong tendency in the occurrence of TCs. To determine whether this phenomenon has actually occurred, a statistical change-point analysis was applied to this time series (blue line) using a 9-year sliding window. The largest absolute value of the t-value appears in 1998, indicating a shift in the climate regime around this year. The average longitude of TC genesis was 136.9°E during 1979–1997 and 132.3°E during 1998–2020, with a difference of 3.6° between the two periods. This difference was significant at the 95%

confidence level. This implies that TCs occurred farther west by approximately 300–400 km during 1998–2020 than during 1979–1997. In the next section, the average difference between the periods 1998–2020 and 1979–1997 is analyzed to determine why more recent TCs have occurred farther west of the WNP than before.

4. Large-scale environment and atmospheric circulation

First, we analyzed the difference in TC genesis frequency between the two periods (Fig. 2a). TCs during 1998–2020 had a strong tendency to occur mainly in the sea near the Philippines and in the South China Sea. However, during 1979–1997, TCs had a higher preference in the eastern waters of the WNP. That is, recently, TCs occurred more often to the western side of the WNP. The TC passage frequency indicates that the frequency of TC migration along the East Asian coast is higher (Fig. 2b); therefore, East Asian coastal countries have the increased TC-related risk.

The reason why recent TCs have occurred west of the WNP can be found from GPI field. A positive anomaly was located in the northern region as well as in the western region of the WNP (Fig. 3a). Conversely, a negative anomaly was located south of 20°N and east of 150°E. As a proxy for deep convection, OLR is shown in Fig. 3b where a negative OLR anomaly is distributed in the western region of the WNP (relative to 140°E), and a positive anomaly is in the eastern part of the WNP. This means that during 1998–2020, convection was more active in the western WNP than during 1979–1997. The precipitable water shows the similar results as those of the GPI (Fig. 3c). Except for the eastern seas of the WNP, most of the analyzed areas showed a positive anomaly. Rainfall field indicates a spatial distribution opposite to that of the OLR (Fig. 3d); the region west of 140°E shows the positive anomaly, while the region east of 140°E shows the negative anomaly.

The occurrence of TCs in more or less farther western area of the WNP during 1998–2020 can also be attributed to environmental factors affecting the occurrence of TCs. For example, the 600-hPa relative humidity (RH600) shows that the region west of 150°E has a positive anomaly, while the region east of 150°E has a negative anomaly (Fig. 3e). The VWS field shows that the negative anomaly south of 10°N is located farther west than the positive anomaly at 10°–20°N (Fig. 3f). Figure 3g shows a positive low-level relative vorticity anomaly located slightly farther northwest than the negative anomaly in the WNP. The 850-hPa horizontal divergence shows anomalous convergence over the western region of the WNP, while anomalous divergence over the eastern region of the WNP (Fig. 3h). All these indicate that convection during 1998–2020 is more active in the west of the WNP than during 1979–1997

To examine whether the climate regime shift occurred in 1998 in all of the above variables, statistical change-point analysis for GPI, OLR, and RH600 was applied to the area-averaged time series in the western (0°–25°N, 100°–140°E) and eastern regions (0°–25°N, 140°–180°E) of the WNP (Fig. 4), where 140° E is the longitude of dividing the opposite anomalies in the OLR field (Fig. 3b). Trends for GPI and RH600 averaged in the western WNP shows an increasing trend, but OLR shows a decreasing trend (these trends were significant at the 95% confidence level), indicating that the large-scale environment favorable for the occurrence of TCs in the western region of the WNP has formed in recent years. The statistical change-point applied to the time series reveals that the largest absolute value of the *t*-value existed for 1998 for all three variables. Thus, the supportive environments for the formation of TCs have been present in the western WNP since 1998. Meanwhile, environments unfavorable for the occurrence of TCs have been formed in the eastern WNP (the area-averaged GPI and RH600 decreased, while OLR increased). This region also shows the largest absolute value of the *t*-value occurring in 1998, indicating that fewer TCs have occurred in the eastern region of the WNP since 1998.

The changes in the large-scale environments, shown above, between 1998–2020 and 1979–1997 can be identified in the difference in the 850-hPa stream flow between the two periods (Fig. 5a). Whereas the large anomalous anticyclonic circulation exists in the WNP region, an anomalous cyclonic circulation is located in East Asia. This is the west-low–east-high spatial pressure pattern. Owing to the huge anomalous anticyclonic circulation located in the WNP during 1998–2020, TCs could not develop in the eastern WNP but rather occurred in the western WNP. In addition, from this anomalous pressure pattern, the eastern coast of China and the Korean peninsula are affected by anomalous southerlies; these steering flows affect the TC track shown in Fig. 2b, in such a way that during 1998–2020, TCs could mainly affect the Korean Peninsula from the Philippines region through the east coast of China. The tendency for TCs to occur to the west during 1998–2020 was identified in the longitudinal position of monsoon troughs in the two periods (represented by red lines in Figs. 5b and 5c). The monsoon trough appeared only up to 125°E during 1998–2020 (Fig. 5b) but expanded eastward to approximately 140°E during 1979–1997 (Fig. 5c); the latter situation supports the development of TC to more eastern side of the WNP.

Consistent with the OLR field shown in Fig. 3b, for the latitudinal range of 100°–140°E the meridional circulation pattern (left panel of Fig. 6a) shows the anomalous upward motions over the region where TCs mainly occur (0°–28°N), whereas the anomalous downward motions are formed in the mid-latitude zone of East Asia (30°–40°N); in contrast, for the domain of 140°–180°E, the anomalous downward motions develop strongly at 5°–20°N, while anomalous upward motions are formed at 20°–40°N (right panel of Fig. 6a). This property is also manifested in the longitude–height plot (Fig. 6c). The relative humidity anomalies (Fig. 6b) shows roughly the consistent result with other variables. These atmospheric circulations and moisture conditions are directed toward the formation of more TCs in the western region of the WNP during 1998–2020.

The TUTT is an elongated trough stretching from the mid-latitude to the tropics (red lines in Figs. 7a and b) and since it induces a large amount of VWS, tropical disturbances can be subdued. However, in the vicinity of TC center (usually to the northeast of it), TUTT can help ventilate the upper-level air so that TC can develop and/or intensify (Barry and Carlton 2001). Figures 7a and 7b show evidently that the TUTT developed westward to 155°E during 1998–2020 but contracted eastward to 165°E during 1979–1997, indicating the favorable environment for more TCs to develop over western WNP. The longitudinal location of the TUTT averaged in June–October was analyzed each year (Fig. 7c). The annual mean east–west shift of the TUTT is measured by dividing the boundary between the easterly and westerly winds in the trough (zero contour of zonal wind speed over 5°–20°N). The longitudinal location of the TUTT shows a decreasing trend, which is significant at the 95% confidence level. There is a clear in-phase relationship between the locations of the TC genesis and TUTT longitudes; a positive correlation of 0.62 (0.59 if the linear trends are removed) was found between the two variables. The statistical change-point analysis (Fig. 7d) shows that the largest absolute value of the *t*-value occurred in 1998, indicating the interdecadal variation of the TUTT longitudes.

5. Teleconnection related to SST variation

The difference in SST between the two periods (Fig. 8a) indicates a warm anomaly over the western region of the WNP and a cold one over the eastern region. This spatial distribution of SST anomalies causes TCs during 1998–2020 to occur in the western WNP. In fact, the whole SST field is typical of the cold PDO pattern and its index shows a decreasing trend until recently (Fig. 8b). This PDO time series has a correlation of 0.52 (0.49 if the linear trends are removed) with that of TC genesis longitudes averaged from June to October. This implies that the lower (higher) the PDO index is, the more TCs is formed in the western (eastern) region of the WNP. The statistical change-point analysis (Fig. 8c) demonstrates the largest absolute value of the *t*-value in 1998, indicating the interdecadal variation of the PDO index time series.

The difference in 500-hPa omega between the two periods (Fig. 9a) indicates the similar result. Over the latitudinal area of 0°–10°N, anomalous upward motions developed west of 160° E, while anomalous downward motions east of 160°E, implying the environment supportive of the formation of more TCs in the western WNP. The dipole pattern exhibits the strengthening of the Walker circulation after 1998. To examine whether Walker circulation is correlated with the location of TC genesis longitude, the average Walker circulation index during June–October is obtained by using the method of Vecci et al. (2006). This index shows the increasing trend until recently, but this trend is not statistically significant (Fig. 9b). In addition, an out-of-phase relationship between the two variables was clear (r = –0.68), implying that the stronger (weaker) the Walker circulation is, the higher the possibility is of TCs occurring on the western (eastern) side of the WNP. The Walker circulation index also produces the largest *t*-value at 1998, as before.

5. Summary

The statistical change-point analysis was applied to the TC genesis longitude averaged from June to October in each year from 1979–2020. It was found that the longitude of TC genesis has shifted to the west since 1998. The average longitude location during 1979–1997 was 136.9° E, whereas it was 132.3°E during 1998–2020, a difference of 300–400 km in distance between the two periods. The present study investigates the possible mechanisms of this shift.

The recent trend for TCs to occur in the western WNP was confirmed by many thermodynamic and dynamics variables. Here, positive precipitation, GPI, and 600-hPa relative humidity (OLR) anomalies were observed in the western (eastern) WNP. In contrast, negative precipitation, GPI, and 600-hPa relative humidity (OLR) anomalies were located east (west) of 140°E. All these indicate that convection was more active in the western area of the WNP during 1998–2020 than during 1979–1997. The VWS anomalies showed that the negative anomalies below 10°N were located further west than the positive anomalies at 10°–20°N. The 850-hPa relative vorticity anomalies also showed that positive anomalies were located farther northwest than were the negative anomalies in the WNP.

The changes in the large-scale environment between 1998–2020 and 1979–1997 as shown above, could be confirmed by the difference in the 850-hPa stream flow between the two periods. The large anomalous anticyclonic circulation existed in the WNP, while the anomalous cyclonic circulation existed in East Asia. Owing to the huge anomalous anticyclonic circulation located in the WNP, TCs during 1998–2020 could not occur in the eastern area of the WNP but rather occurred in the western side. This was confirmed by the longitudinal location of development of monsoon troughs during the two periods; the monsoon troughs only developed up to 125°E during 1998–2020 but developed eastward to approximately 140°E during 1979–1997.

Vertical meridional circulations and relative humidity averaged over 100°–140°E and 140°–180°E, respectively, were also analyzed. In the vertical meridional circulation averaged at 100°–140°E (140°–180°E), anomalous upward flows developed (at 20°–40°N) in the region where TCs mainly occurred, whereas anomalous downward flows were formed (at 5°–20°N) in the mid-latitude zone of East Asia. In addition, positive relative humidity anomalies were observed at 0°–40°N.

TUTTs developed more westward during 1998–2020 than during 1979–1997. The TUTT time series show the climate regime shift in 1998, and since 1998, there has been a strong tendency toward a westward shift of the TUTT.

The differences in SST between the two periods shows the warm (cold) anomaly over the western (eastern) region of the WNP, and, considering the midlatitude anomalies together, this SST anomaly field is the characteristic pattern of cold PDO phase. The difference in the 500-hPa omega between the two periods demonstrates the strengthening of the Walker circulation, which also showed a climate regime shift in 1998 (Fig. 10).

This study showed that TC genesis longitude was shifted westward in the WNP during the cold PDO phase. The precise physical mechanisms can be verified using a series of sensitivity tests using coupled climate model, which will be pursued as a future work. As shown above, more TCs develop over the western area of the WNP in recent years, implying the higher risk of natural hazard along the coastal countries of East Asia, which requires increased precaution in those areas.

Acknowledgements

This work is supported by a National Research Foundation of Korea (NRF) grant funded by the Korean government (MSIP) (No. NRF-2020R1A2C2009414) and the Korea Meteorological Administration (KMA) Research and Development Program under Grant KMI2021–01410.

References

Barry RG, Carleton AM (2001) Synoptic and dynamic climatology. Psychology Press. p. 519. ISBN 978-0-415-03115-8.

Camargo SJ, Emanuel KA, Sobel AH (2007) Use of a genesis potential index to diagnose ENSO effects on tropical cyclone genesis. IRI Technical Report 07-01, 45 pp., International Research Institute for Climate Prediction, Palisades, NY

Camargo SJ, Sobel AH (2005) Western North Pacific tropical cyclone intensity and ENSO. J Clim 18:2996–3006

Cao X, Liu Y, Wu R, Bi M, Dai Y, Cai Z (2019) Northwestwards shift of tropical cyclone genesis position during autumn over the western North Pacific after the late 1990s. Int J Climatol 40:1885-1899

Chia HH, Ropelewski CF (2002) The interannual variability in the genesis location of tropical cyclones in the Northwest Pacific. J Clim, 15:2934– 2944.

Deng K, Yang S, Ting M, Hu C, Lu M (2018) Variations of the mid-Pacific trough and their relations to the Asian-Pacific-North American climate: Roles of tropical sea surface temperature and Arctic sea ice. J Clim 31:2233-2252

Enfield, D. B., Mestas-Nuñez, A. M., and Paul, J. T. (2001). The Atlantic multidecadal oscillation and its relation to rainfall and river flows in the continental us. Geophys Res Lett 28 (10):2077–2080. doi:10.1029/2000gl012745

Gray WM (1984) Atlantic seasonal hurricane frequency Part I: El Niño and 30 mb quasi-biennial oscillation influences Mon Wea Rev 112:1649-1668

Hastings RA (1990) Southern Oscillation influences on tropical cyclone activity in the Australian/south-west Pacific region. Int J Climatol 10:291-298

Hu C, Zhang C, Yang S, Chen D, He S (2018) Perspective on the northwestward shift of Autumn tropical cyclogenesis locations over the western North Pacific from shifting ENSO. Clim Dyn 51:2455-2465

Huang R, Huangfu J, Wu L, Feng T, Chen G (2016) Research on the interannual and interdecadal variabilities of the monsoon trough and their impacts on tropical cyclone genesis over the western North Pacific. J Tropic Meteorol 32:767–785 (In Chinese)

Huangfu J, Huang R, Chen W, Feng T, Wu L (2017) Interdecadal variation of tropical cyclone genesis and its relationship to the monsoon trough over the western North Pacific. Int J Climatol 37:3587–3596

Kanamitsu M, W Ebisuzaki, Woollen J, Yang SK, Hnilo JJ, Fiorino M, Potter GL (2002) NCEP-DOE AMIP-II Reanalysis (R-2). Bull Amer Meteor Soc 83:1631-1643

Kim HK, Seo KH (2016) Cluster analysis of tropical cyclone tracks over the western North Pacific using a self-organizing map. J Clim 29:3731-3751

Kim HM, Webster PJ, Curry JA (2011) Modulation of North Pacific tropical cyclone activity by three phases of ENSO. J Clim 24:1839–1849

Kubota H, Chan JCL (2009). Interdecadal variability of tropical cyclone landfall in the Philippines from 1902 to 2005. Geophy Res Lett, 36(12). https://doi.org/10.1029/2009gl038108

Lander MA (1994) An exploratory analysis of the relationship between tropical storm formation in the western North Pacific and ENSO. Mon Wea Rev 122:636–651

Lee M, Kim T, Cha DH, Min SK, Park DSR, Yeh SW, Chan JCL (2021). How does Pacific Decadal Oscillation affect tropical cyclone activity over Far East Asia? Geophy Res Lett, 48, e2021GL096267. https://doi.org/10.1029/

Liebmann B, Smith CA (1996) Description of a complete (interpolated) outgoing longwave radiation dataset. Bull Amer Meteor Soc 77:1275–1277

Liu KS, Chan JCL (2008). Interdecadal variability of western North Pacific tropical cyclone tracks. J Clim 21(17):4464– 4476.

Liu KS, Chan JC (2013). Inactive period of western North Pacific tropical cyclone activity in 1998–2011. J Clim 26(8):2614– 2630.

Mantua NJ, Hare SR, Zhang Y, Wallace JM, Francis RC (1997) A Pacific interdecadal climate oscillation with impacts on salmon production. Bull Amer Meteor Soc 78:1069–1079.

McCabe GJ, Palecki MA, Betancourt JL (2004) Pacific and Atlantic Ocean influences on multidecadal drought frequency in the United States. *Proc. Natl. Acad. Sci. U.S.A.* 101 (12), 4136–4141. doi:10.1073/pnas.0306738101

Smith TM, Reynolds RW, Peterson TC, Lawrimore J (2008) Improvements to NOAA's historical merged land-ocean surface temperature analysis (1880-2006). J Clim 21:2283-2296

Scoccimarro E, Villarini G, Gualdi S, Navarra A (2021) The Pacific Decadal Oscillation Modulates Tropical Cyclone Days on the Interannual Timescale in the North Pacific Ocean. J Geophy Res 126:e2021JD034988

Sutton RT, Dong B (2012) Atlantic Ocean influence on a shift in European climate in the 1990s. Nat. Geosci. 5 (11):788–792. doi:10.1038/ngeo1595

Sutton RT, Hodson DLR (2005) Atlantic Ocean forcing of north American and European summer climate. Science 309 (5731):115–118. doi:10.1126/science.1109496

Vecchi GA, Soden BJ, Wittenberg AT, Held IM, Leetmaa A, Harrison MJ (2006) Weakening of tropical Pacific atmospheric circulation due to anthropogenic forcing. Nature 441:73–

76

Wang B and Chan JCL (2002) How strong ENSO events affect tropical storm activity over the western North Pacific. J Clim 15:1643– 1658

Wang C, and Lee SK (2009) Co- variability of tropical cyclones in the North Atlantic and the eastern North Pacific. Geophys Res Lett 36:L24702. doi:10.1029/2009gl041469

Wang C, Li C, Mu M, Duan W (2013) Seasonal modulations of different impacts of two types of ENSO events on tropical cyclone activity in the western North Pacific. Clim Dyn 40:2887–2902

Wang C, Wu L (2016) Interannual shift of the tropical upper-tropospheric trough and its influence on tropical cyclone formation over the western North Pacific. J Clim 29:4203–4211

Wang X, Liu H (2016) PDO modulation of ENSO effect on tropical cyclone rapid intensification in the western North Pacific. Clim Dyn 46:15-28

Wilks DS (1995) Statistical methods in the atmospheric sciences. Academic Press, 467 pp

Wingo MT, Cecil DJ (2010) Effects of vertical wind shear on tropical cyclone precipitation. Mon Wea Rev 138:645-662

Yang L, Chen S, Wang C, Wang D, Wang X (2018). Potential impact of the pacific decadal oscillation and sea surface temperature in the tropical Indian Ocean–Western Pacific on the variability of typhoon landfall on the China coast. Clim Dyn, 51(7):2695– 2705

Zhao H, Wu L, Zhou W (2010) Assessing the influence of ENSO on tropical cyclone prevailing tracks in the western North Pacific. Adv Atmos Sci 27:1–11

Zhou W, Li C, Wang X (2007). Possible connection between Pacific oceanic interdecadal pathway and East Asian winter monsoon. Geophy Res

Lett, 34(1). https://doi.org/10.1029/2006gl027809

List of Figure

Fig. 1. Time series of TC genesis longitude averaged for June–October (JJASO) (red line with dot) and the statistical change-point profile (blue line).

Fig. 2. Differences in (a) TC genesis frequency (TCGF) and (b) TC passage frequency (TCPF) between 1998–2020 and 1979–1997 in JJASO. In (a) and (b), the small squares inside the circles indicate that the differences are significant at the 95% confidence level. TC, tropical cyclone.

Fig. 3. Composite differences in (a) GPI, (b) OLR, (c) precipitable water, (d) rainfall, (e) 600-hPa relative humidity (RH), (f) vertical wind shear (VWS), (g) 850-hPa relative vorticity, and (h) 850-hPa horizontal divergence between 1998–2020 and 1979–1997 in JJASO. Hatched areas are significant at the 95% confidence level.

Fig. 4. Time series of GPI, OLR, 600-hPa RH averaged for the western area (0°–25°N, 100°–140°E; left panel) and the eastern area (0°–25°N, 140°–180°E; right panel) of the western North Pacific in JJASO.

Fig. 5. (a) Composite difference in stream flows at 850-hPa and composites of (b) 850-hPa geopotential height (GPH) for 1998–2020 and (c) 850-hPa GPH for 1979–1997 in JJASO. In (a), gray-shaded areas are significant at the 95% confidence level.

Fig. 6. Composite differences of latitude–pressure cross-section of (a) vertical velocity (contours) and meridional circulation (vectors), (b) relative humidity averaged along 100°–140°E (left panel) and 140°–180°E (right panel) between 1998–2020 and 1979–1997 in JJASO. The values of vertical velocity are multiplied by −100. Hatched areas are significant at the 95% confidence level, and shaded areas denote negative values. Contour intervals are 3^{-2}hPa s^{-1} and 1% for vertical velocity and relative humidity, respectively.

Fig. 7. Tropical upper tropospheric trough (TUTT) averaged for (a) 1998–2020 and (b) 1979–1997 in JJASO and time series of (c) TC genesis longitude, TUTT longitude, and (d) *t*-value of the TUTT longitude.

Fig. 8. (a) Composite difference in SST between 1998–2020 and 1979–1997 in JJASO. Time series of (b) TC genesis longitude and Pacific Decadal Oscillation (PDO) index in JJASO and (c) *t*-value on PDO index. In (a), hatched areas are significant at the 95% confidence level. SST, sea surface temperature; TC, tropical cyclone.

Fig. 9. (a) Composite difference in 500-hPa omega in JJASO and time series of (b) TC genesis longitude and Walker circulation index and (c) *t*-value on Walker circulation index. In (a), hatched areas are significant at the 95% confidence level. TC, tropical cyclone.

Fig. 10. Schematic diagram of SST anomalies in cold PDO phase in post-1998. When a cold PDO phase occurs, WNP represents warm SST anomalies and central Pacific forms cold SST anomalies. Then, anomalous forward flows occur in the WNP and anomalous downward flows are formed in central Pacific and then Walker circulation enhances. Eventually, TC genesis longitude is shifted westward in the WNP.

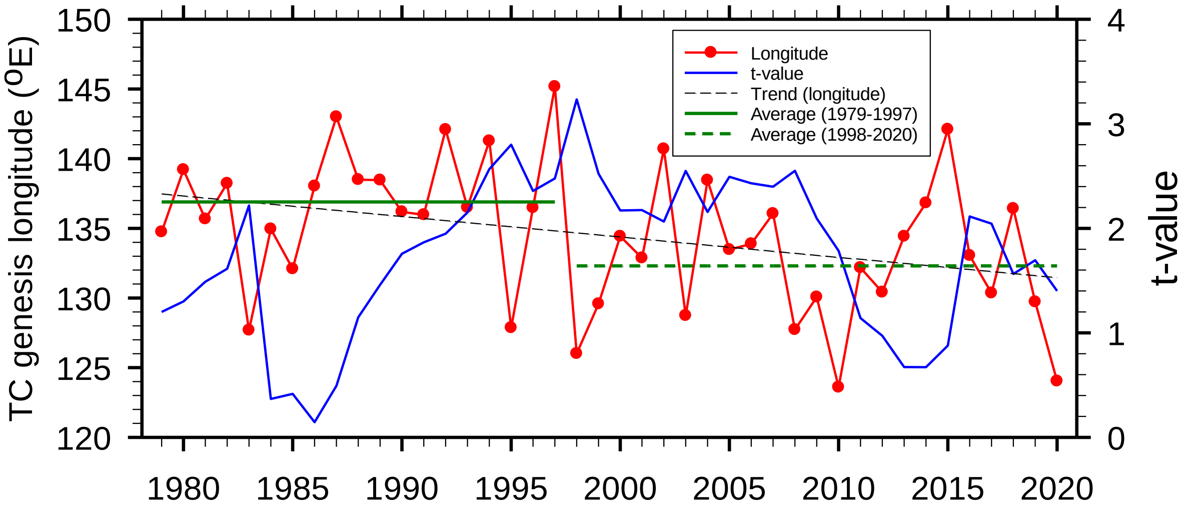

Fig. 1. Time series of TC genesis longitude averaged for June–October (JJASO) (red line with dot) and the statistical change-point curve (blue line).

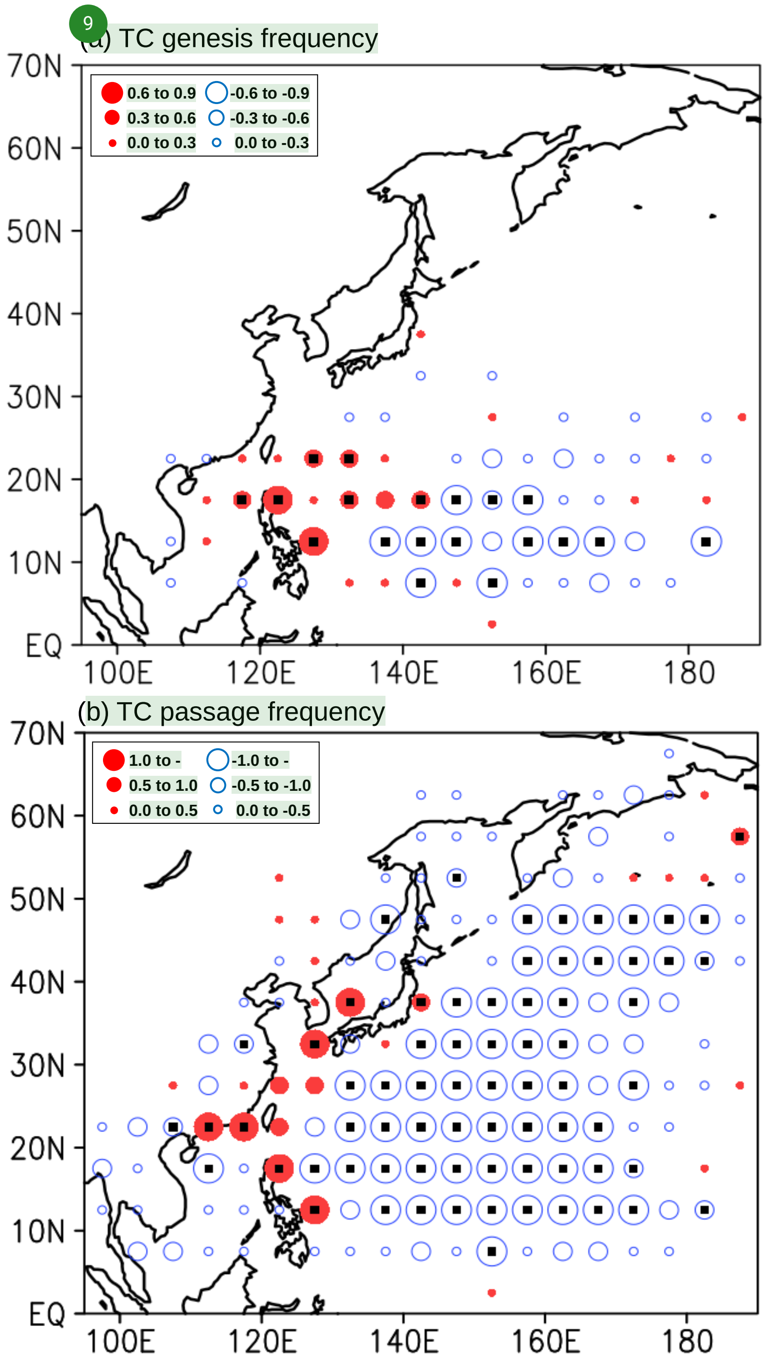

Fig. 2. Differences in (a) tropical cyclone (TC) genesis frequency (TCGF) and (b) TC passage frequency (TCPF) between 1998–2020 and 1979–1997 in JJASO. In (a) and (b), the small squares inside the circles indicate that the differences are significant at the 95% confidence level.

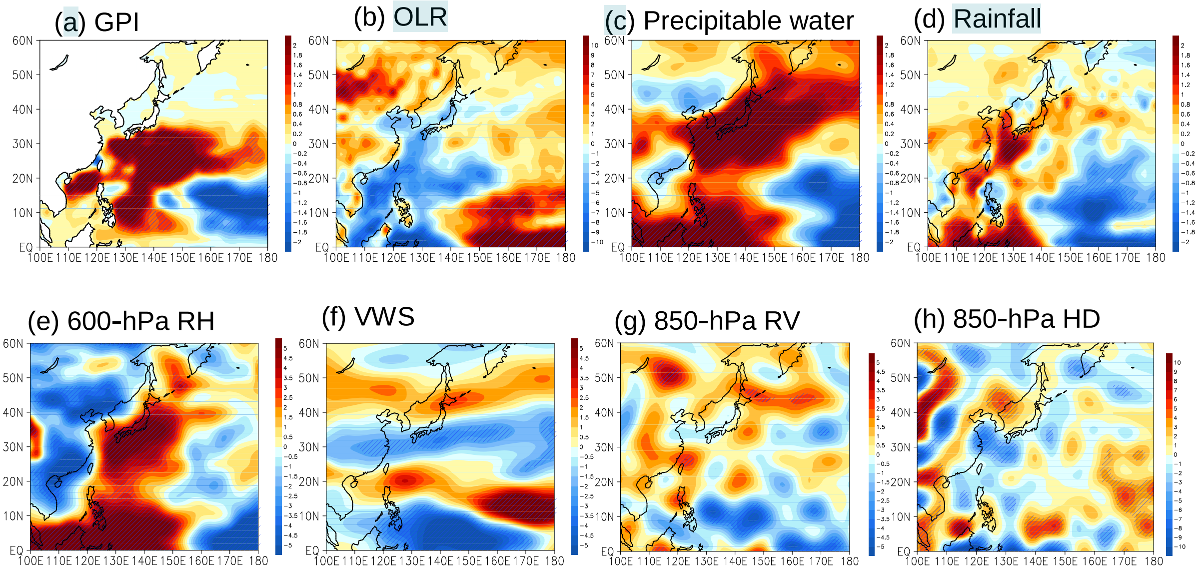

Fig. 3. Composite differences in (a) GPI, (b) OLR, (c) precipitable water, (d) rainfall, (e) 600-hPa relative humidity (RH), (f) vertical wind shear (VWS), (g) 850-hPa relative vorticity, and (h) 850-hPa horizontal divergence between 1998–2020 and 1979–1997 in JJASO. Hatched areas are significant at the 95% confidence level.

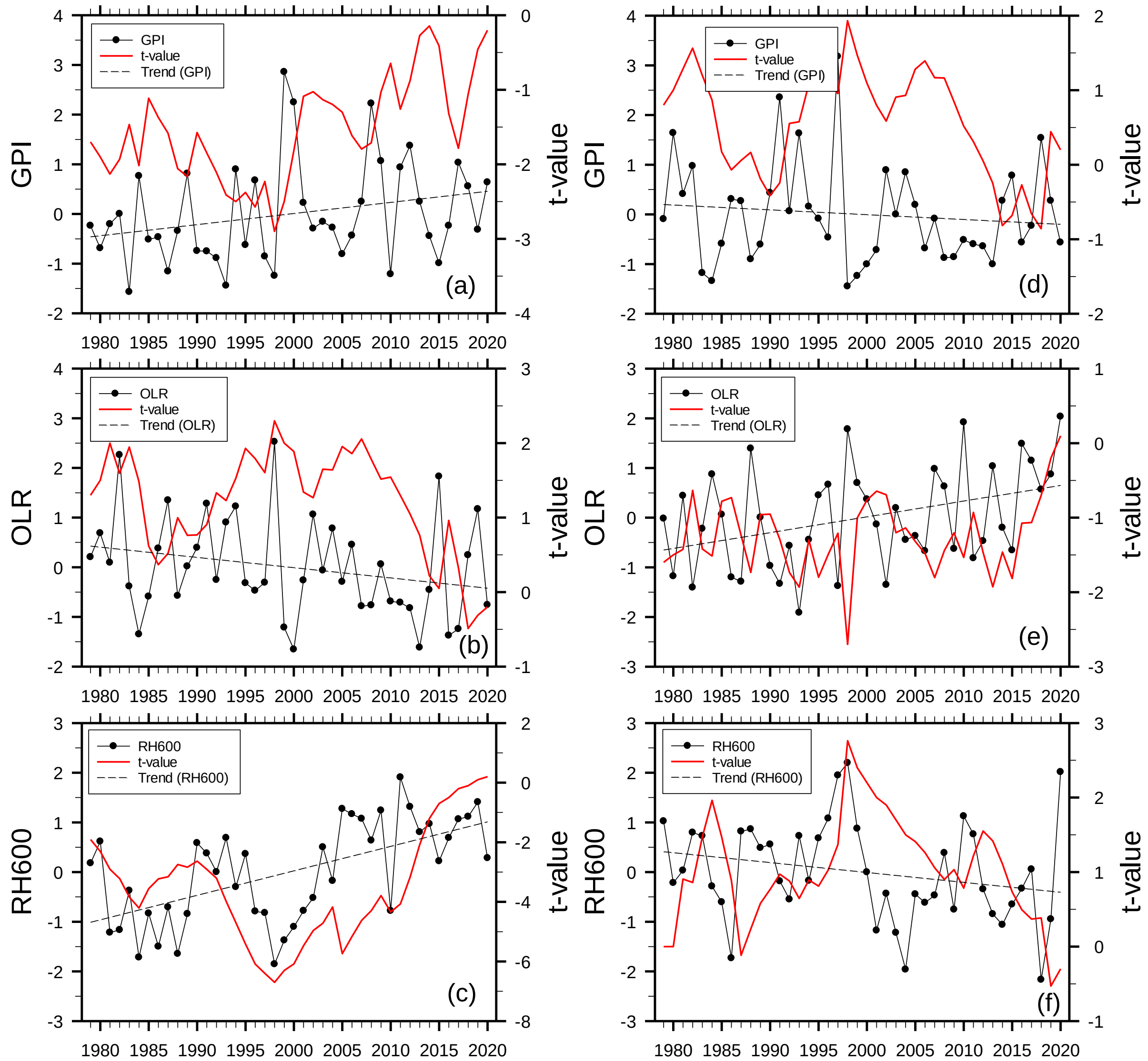

Fig. 4. Time series of GPI, OLR, 600-hPa RH averaged for the western area (0°–25°N, 100°–140°E; left panel) and the eastern area (0°–25°N, 140°–180°E; right panel) of the western North Pacific in JJASO.

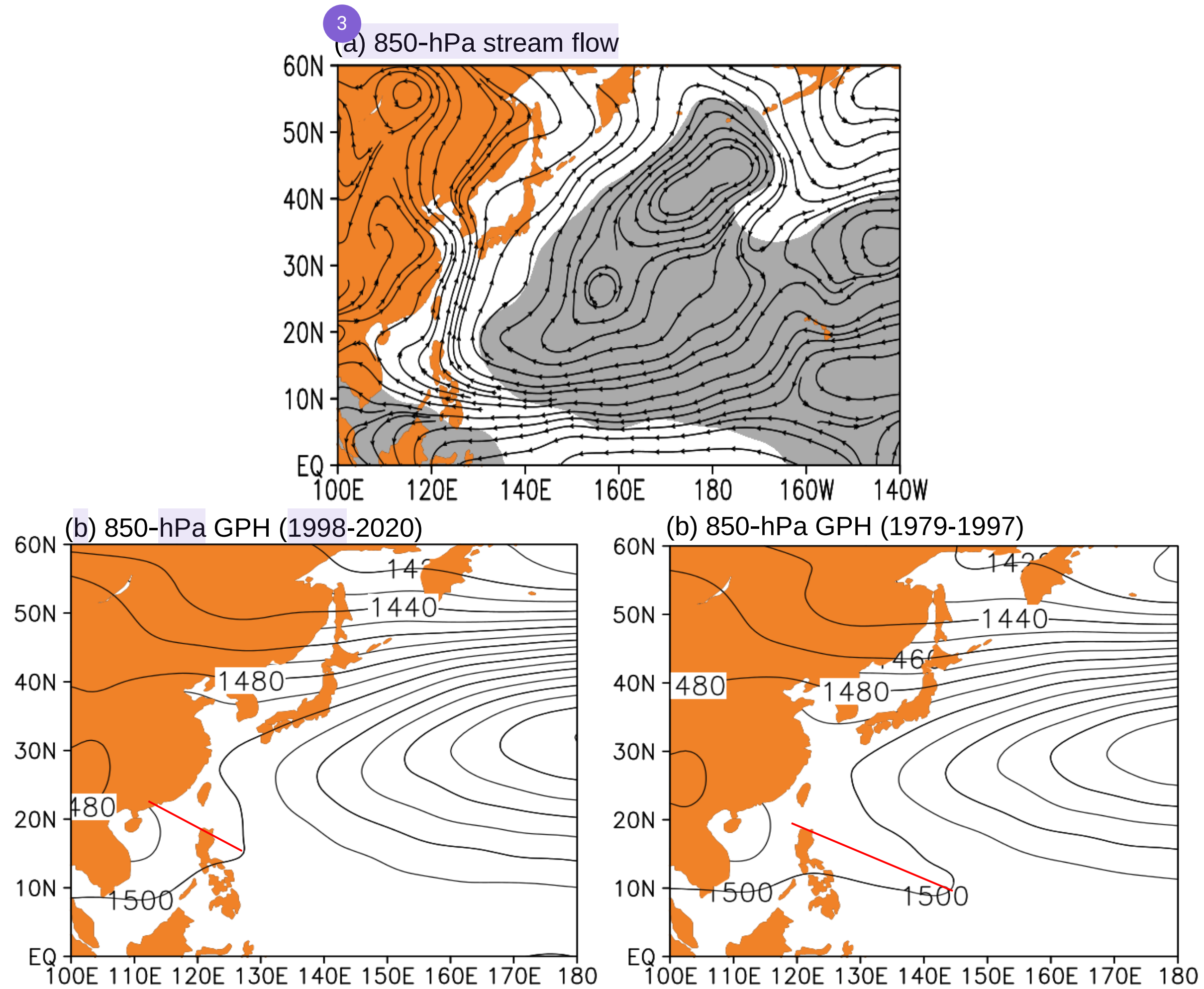

Fig. 5. (a) Composite difference in stream flows at 850-hPa and composites of (b) 850-hPa geopotential height (GPH) for 1998–2020 and (c) 850-hPa GPH for 1979–1997 in JJASO. In (a), gray-shaded areas are significant at the 95% confidence level.

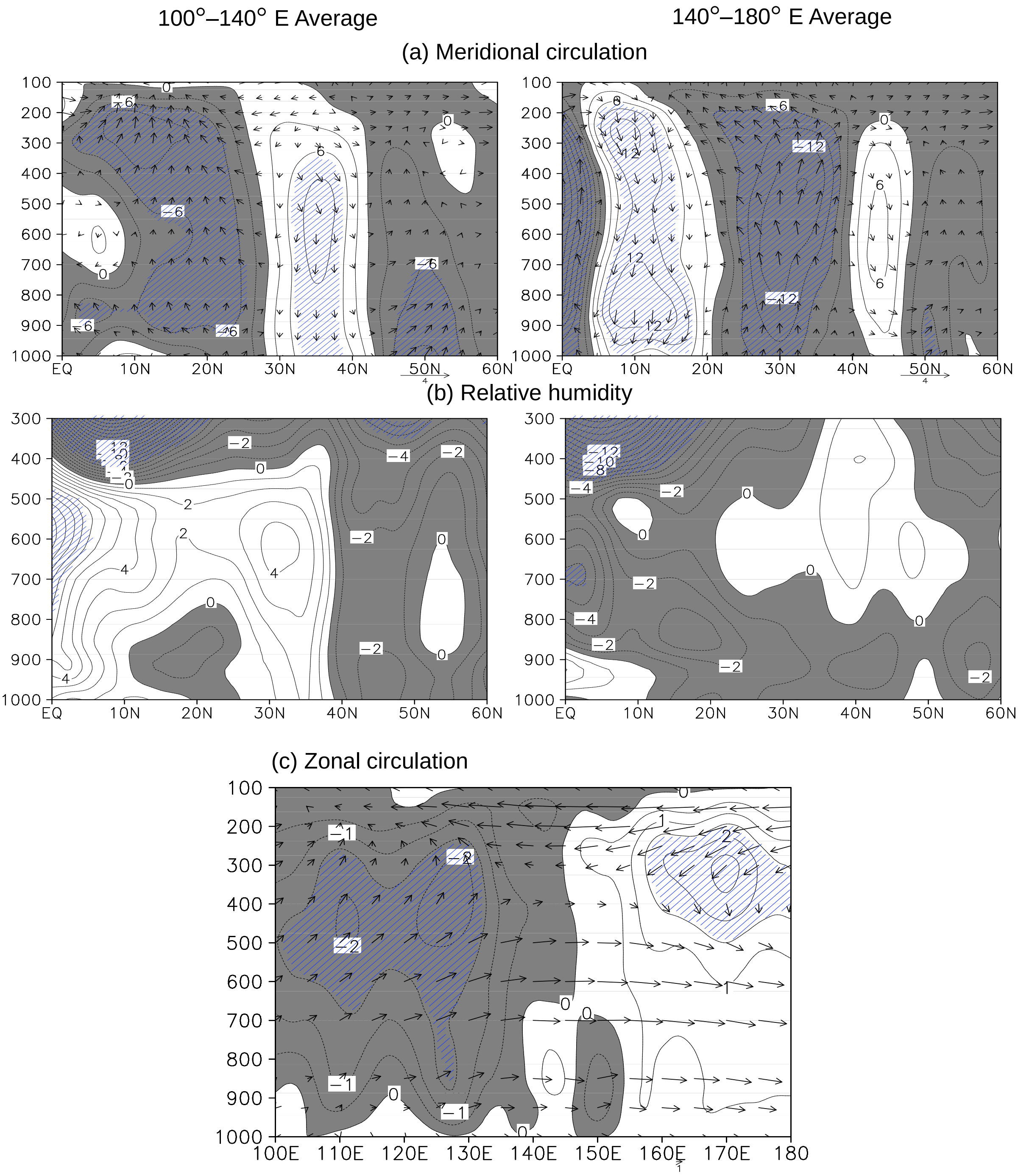

Fig. 6. Composite differences of latitude–pressure cross-section of (a) vertical velocity (contours) and meridional circulation (vectors), (b) relative humidity averaged along 100°–140°E (left panel) and 140°–180°E (right panel) between 1998–2020 and 1979–1997 in JJASO. The values of vertical velocity are multiplied by −100. Hatched areas are significant at the 95% confidence level, and shaded areas denote negative values. Contour intervals are 3^{-2}hPa s^{-1} and 1% for vertical velocity and relative humidity, respectively.

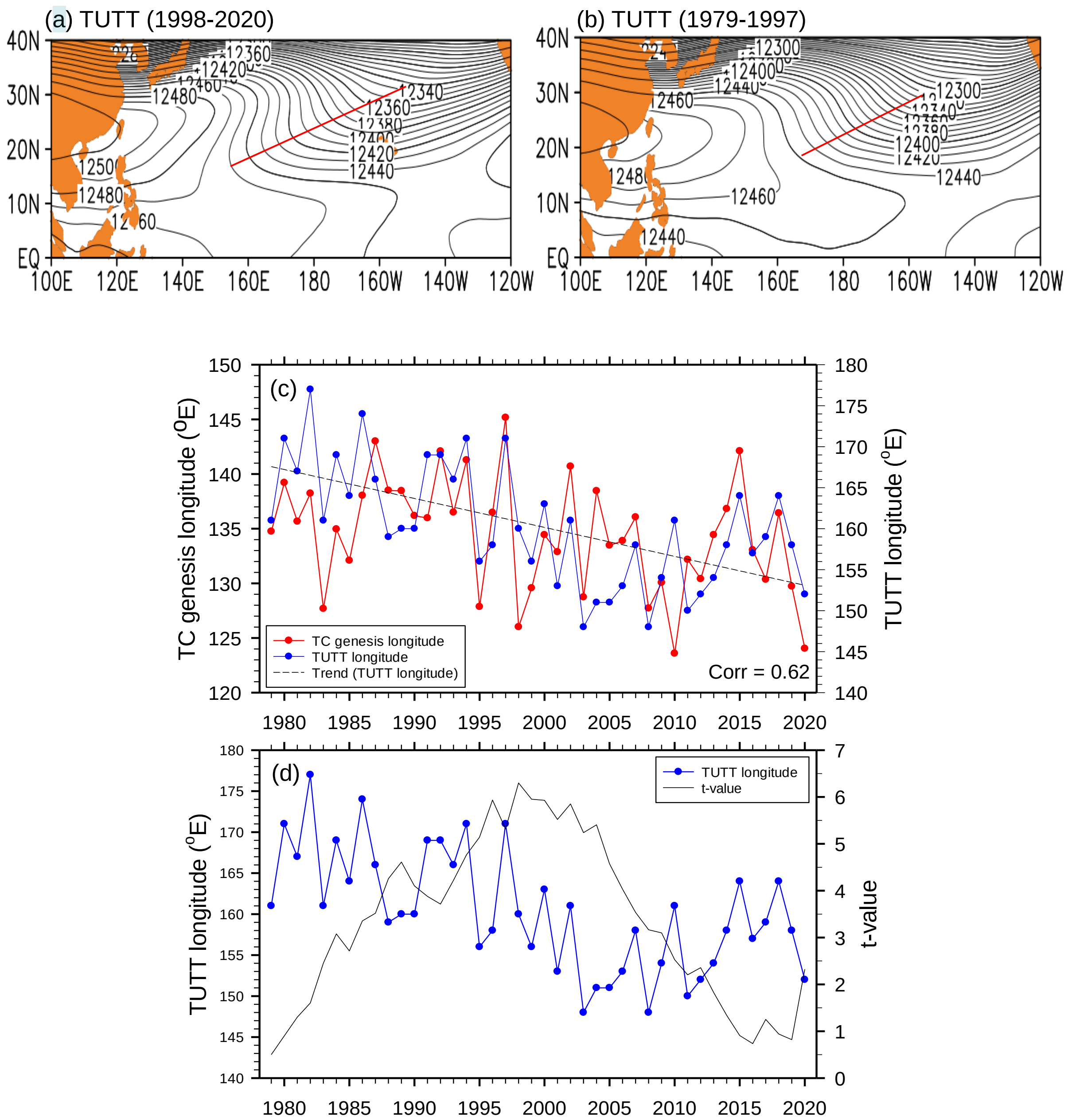

Fig. 7. Tropical upper tropospheric trough (TUTT) averaged for (a) 1998–2020 and (b) 1979–1997 in JJASO and time series of (c) TC genesis longitude, TUTT longitude, and (d) t-value of the TUTT longitude.

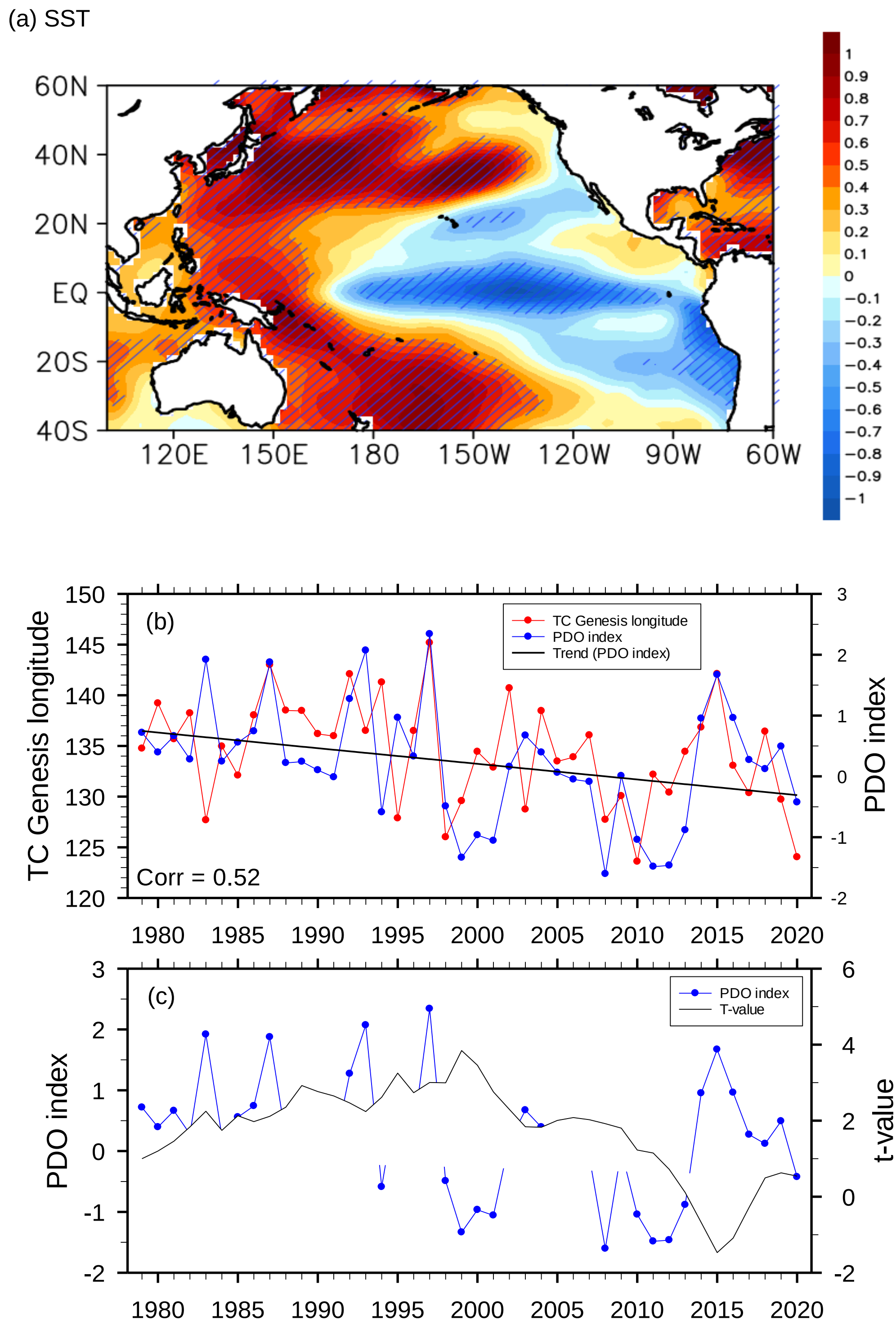

Fig. 8. (a) Composite difference in SST between 1998–2020 and 1979–1997 in JJASO. Time series of (b) TC genesis longitude and Pacific Decadal Oscillation (PDO) index in JJASO and (c) t-value on PDO index. In (a), hatched areas are significant at the 95% confidence level. SST, sea surface temperature; TC, tropical cyclone.

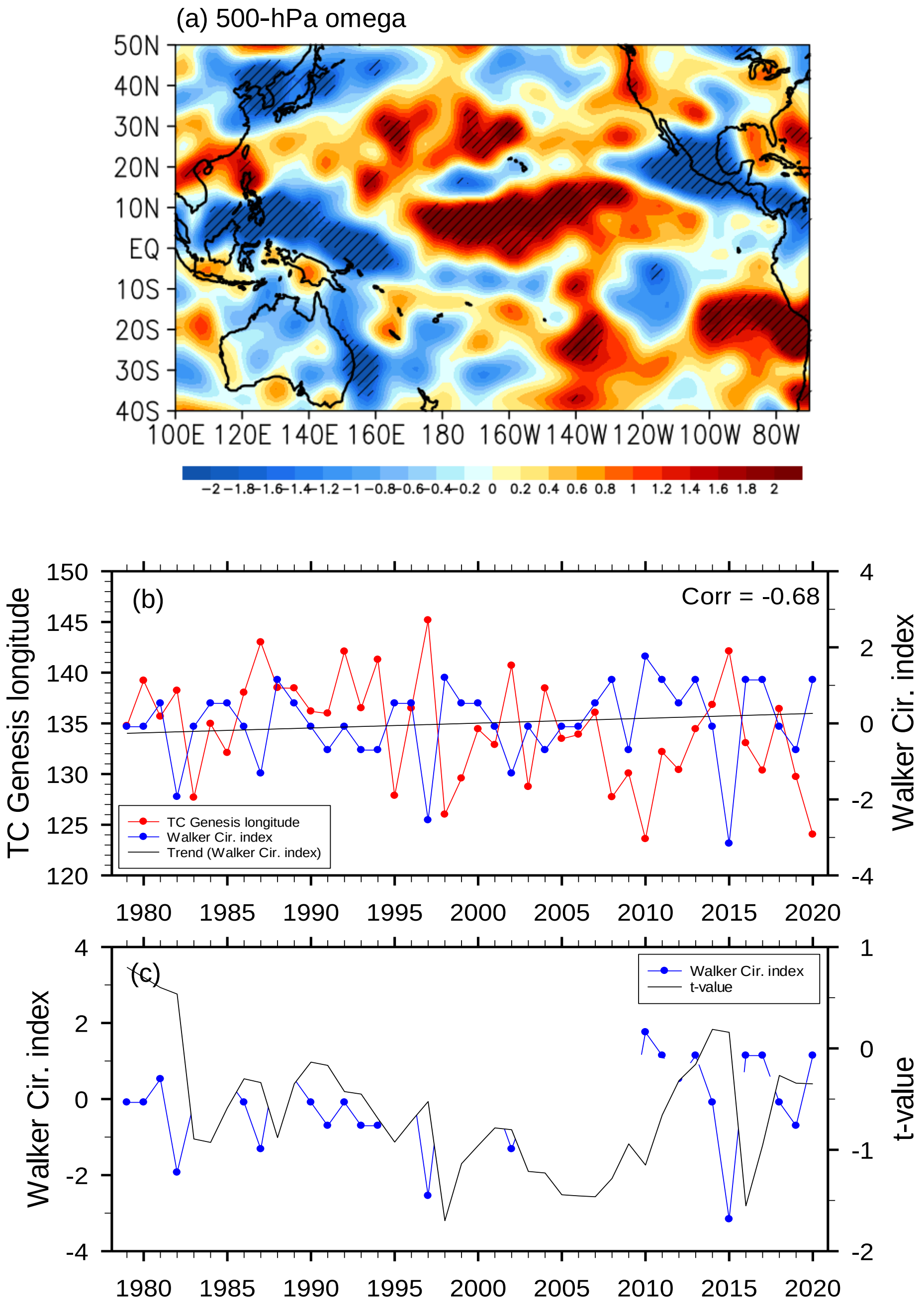

Fig. 9. (a) Composite difference in 500-hPa omega in JJASO and time series of (b) TC genesis longitude and Walker circulation index and (c) t-value on Walker circulation index. In (a), hatched areas are significant at the 95% confidence level. TC, tropical cyclone.

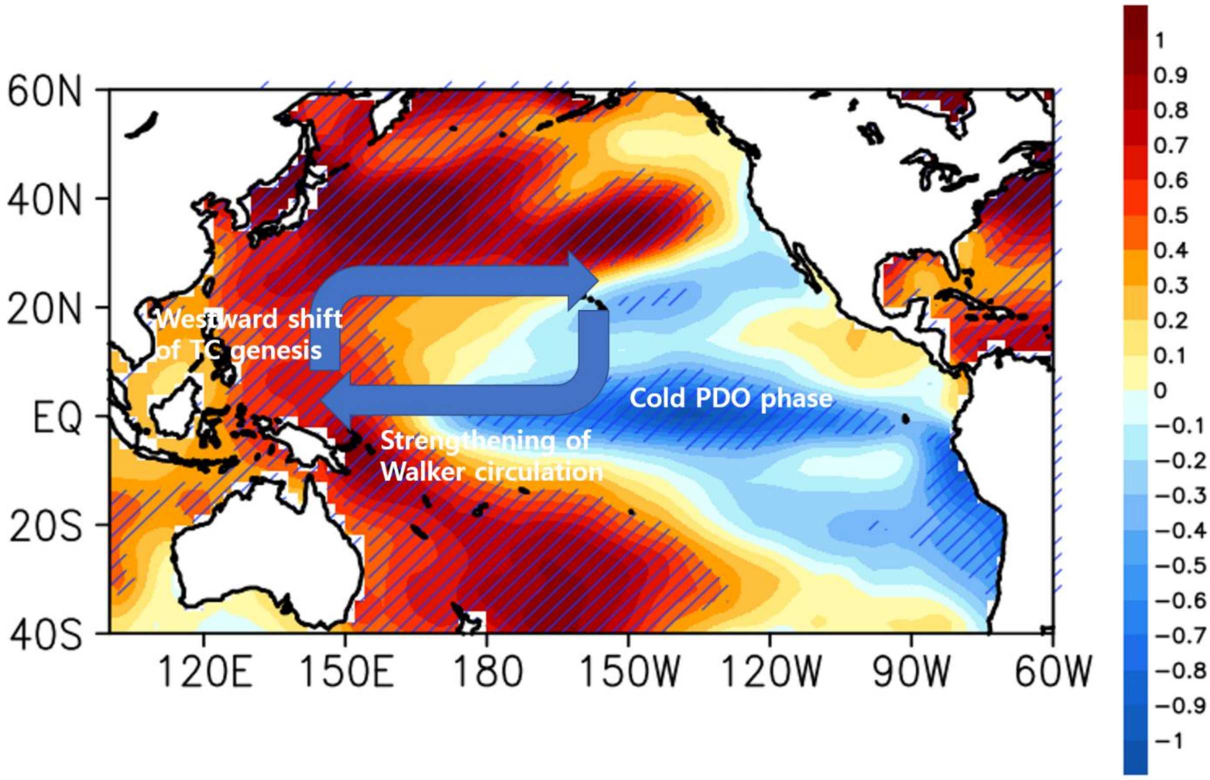

Fig. 10. Schematic diagram of SST anomalies in cold PDO phase in post-1998. During the cold PDO phase, the WNP exhibits warm SST anomalies, whereas the central Pacific shows cold SST anomalies. Then, anomalous upward flows develop in the WNP and anomalous downward flows occur in central Pacific, implying the enhancement of the Walker circulation. Eventually, TC genesis longitude is shifted westward in the WNP.

44% Overall Similarity

Top sources found in the following databases:

- 35% Internet database
- 44% Publications database
- Crossref database
- Crossref Posted Content database
- 0% Submitted Works database

TOP SOURCES

The sources with the highest number of matches within the submission. Overlapping sources will not be displayed.

1	link.springer.com Internet	5%
2	JaeWon Choi, Il-Ju Moon, Boo-Keun Khim. "A possible relationship bet... Crossref	4%
3	climate-prediction.org Internet	3%
4	Yumi Cha, JaeWon Choi, Joong-Bae Ahn. "The interannual synchroniza... Crossref	2%
5	assets.researchsquare.com Internet	2%
6	Jae-Won Choi, Yumi Cha, Taeyun Kim, Hae-Dong Kim. "Interdecadal va... Crossref	1%
7	frontiersin.org Internet	1%
8	Yumi Cha, JaeWon Choi, Joong-Bae Ahn. "Interdecadal changes in the ... Crossref	1%

9	Ki-Seon Choi, Hae-Dong Kim, Sung-Dae Kang, Chang-Sup Shim. "Decre...	Crossref	1%
10	researchsquare.com	Internet	<1%
11	Jae-Won Choi, Yumi Cha, Riyu Lu. "Possible Relationship between Kore...	Crossref	<1%
12	journals.ametsoc.org	Internet	<1%
13	Ki-Seon Choi, Yu-Mi Cha, Sung-Dae Kang, Hae-Dong Kim. "Relationship...	Crossref	<1%
14	iopscience.iop.org	Internet	<1%
15	Daquan Zhang, Lijuan Chen. "Hybrid statistical-dynamical seasonal pre...	Crossref	<1%
16	Jae-Won Choi, Yumi Cha, Sung-Dae Kang, Changsub Shim. "Interdecad...	Crossref	<1%
17	Peng Zhang, Zhiwei Wu, Zhiwei Zhu, Rui Jin. "Promoting seasonal pred...	Crossref	<1%
18	a.tellusjournals.se	Internet	<1%
19	Jae-Won Choi, Yumi Cha, Hae-Dong Kim. "Interdecadal variation of pre...	Crossref	<1%
20	Yumi Choi, Kyung-Ja Ha, Fei-Fei Jin. "Seasonality and El Niño Diversity ...	Crossref	<1%

21	iapjournals.ac.cn Internet	<1%
22	Chalachew Kindie Mengist, Kyong-Hwan Seo, Yong Ha Kim, S. Eswarai... Crossref	<1%
23	Wu, Liguang, Chao Wang, and Bin Wang. "Westward Shift of Western N... Crossref	<1%
24	J. Blunden. "State of the Climate in 2010", Bulletin of the American Met... Crossref	<1%
25	Yumi Cha, JaeWon Choi, Joong-Bae Ahn. "Interdecadal change in the g... Crossref posted content	<1%
26	Choi, Jae-Won, Baek-Jo Kim, Renhe Zhang, Ki-Jun Park, Jeoung-Yun Ki... Crossref	<1%
27	Jae-Won Choi (Ki-Seon Choi), Yumi Cha, Hae-Dong Kim, Riyu Lu. "More... Crossref	<1%
28	Jae-Won Choi, Bin Wang. "Relationship between Antarctic Oscillation a... Crossref	<1%
29	Jun-Hyeok Son, Jae-Il Kwon, Ki-Young Heo. "Weak upstream westerly ... Crossref	<1%
30	Ki-Seon Choi, Yu-Mi Cha, Sung-Dae Kang, Hae-Dong Kim. "Interdecadal... Crossref	<1%
31	klme.nuist.edu.cn Internet	<1%
32	hal.archives-ouvertes.fr Internet	<1%

33	Ki-Seon Choi, Sangwook Park, Ki-Ho Chang, Jong-Ho Lee. "A possible r... Crossref	<1%
34	elib.dlr.de Internet	<1%
35	Jae-Won Choi, Hae-Dong Kim. "The recent increase in central eastern ... Crossref	<1%
36	Xi Cao, Yong Liu, Renguang Wu, Mingyu Bi, Yifeng Dai, Zelin Cai. "North... Crossref	<1%
37	typhoon.or.kr Internet	<1%
38	Liguang Wu, Chao Wang, Bin Wang. "Westward shift of western North ... Crossref	<1%
39	Minkyu Lee, Taehyung Kim, Dong-Hyun Cha, Seung-Ki Min, Doo-Sun R. ... Crossref	<1%
40	Ye, Deng, Huang, Chen. "Comparison of the Madden-Julian Oscillatio... Crossref	<1%
41	Ki-Seon Choi, Hae-Dong Kim, Sung-Dae Kang. "Interdecadal variation o... Crossref	<1%
42	Ki-Seon Choi, Il-Ju Moon. "Changes in tropical cyclone activity that has... Crossref	<1%
43	Ki-Seon Choi, Yu-Mi Cha, Sung-Dae Kang, Hae-Dong Kim. "Interdecadal... Crossref	<1%
44	Ki-Seon Choi, Yumi Cha, Hae-Dong Kim, Sung-Dae Kang. "Possible rela... Crossref	<1%

45	S. Gualdi, E. Scoccimarro, A. Navarra. "Changes in Tropical Cyclone Ac... Crossref	<1%
46	Jae-Won Choi, Hae-Dong Kim. "Possible combined effect of El Niño-So... Crossref	<1%
47	Jae-Won Choi, Hae-Dong Kim. "Relationship of the Southeast Asian su... Crossref	<1%
48	Haikun Zhao, Chunzai Wang. "On the relationship between ENSO and tr... Crossref	<1%
49	Minkyu Lee, Taehyung Kim, Dong-Hyun Cha, Seung-Ki Min, Doo-Sun R. ... Crossref	<1%
50	nature.com Internet	<1%
51	Lakshmi Krishnamurthy, Gabriel A. Vecchi, Rym Msadek, Hiroyuki Mur... Crossref	<1%
52	Ki-Seon Choi, Do-Woo Kim, Hi-Ryong Byun. "Statistical model for seaso... Crossref	<1%
53	Booth, R.K.. "Widespread drought episodes in the western Great Lakes ... Crossref	<1%
54	Jae-Won Choi, Yumi Cha, Jeoung-Yun Kim. "Characteristics of the Non... Crossref	<1%
55	geoscienceletters.springeropen.com Internet	<1%
56	mdpi.com Internet	<1%

57	Kai Zhao, Haikun Zhao, Graciela B. Raga, Ryuji Yoshida, Weiqiang Wan... Crossref	<1%
58	Tzu-Ling Lai, Jau-Ming Chen, Pei-Hua Tan, Jien-Yi Tu, Hui-Shan Chen, ... Crossref	<1%
59	shareok.org Internet	<1%
60	researchgate.net Internet	<1%
61	Ki-Seon Choi, Su-Bin Oh, Hi-Ryong Byun, R. H. Kripalani, Do-Woo Kim. "... Crossref	<1%
62	Wu, Liguang, and Bin Wang. "Assessing Impacts of Global Warming on ... Crossref	<1%
63	Yu, Jinhua, Cheng Chen, Tim Li, Xiaotong Zhao, Huaxing Xue, and Qiyin... Crossref	<1%
64	jmr.cmsjournal.net Internet	<1%
65	Andy Zung-Ching Goh. "Interannual and interdecadal variations of tropi... Crossref	<1%
66	Chaoming Huang, Hailong Liu, Xidong Wang, Hong Li, Zhaoru Zhang, J... Crossref	<1%
67	Chi-Cherng Hong, Ming-Ying Lee, Huang-Hsiung Hsu, Nai-Hsin Lin, Ben... Crossref	<1%
68	Haikun ZHAO, Liguang WU, Weican ZHOU. "Interannual Changes of Tro... Crossref	<1%

69	Haikun Zhao, Liguang Wu, Weican Zhou. "Assessing the influence of th... Crossref	<1%
70	Jae-Won Choi, Hae-Dong Kim. "Negative relationship between Korea la... Crossref	<1%
71	Jianyun Gao, Tim Li. "Factors Controlling Multiple Tropical Cyclone Eve... Crossref	<1%
72	Ki-Seon Choi, Bin Wang, Do-Woo Kim. "Changma onset definition in Ko... Crossref	<1%
73	Ki-Seon Choi, Yu-Mi Cha, Tae-Ryong Kim. "Cluster analysis of tropical c... Crossref	<1%
74	Shuang Li, Ziniu Xiao, Yuchun Zhao. "Combined Effect of PDO and ENS... Crossref	<1%
75	cyberleninka.org Internet	<1%
76	irgu.unigoa.ac.in Internet	<1%
77	kjc.nuist.edu.cn Internet	<1%
78	tao.cgu.org.tw Internet	<1%
79	ideals.illinois.edu Internet	<1%
80	Chalachew Kindie Mengist, Kyong-Hwan Seo. "How Long Can the MJO ... Crossref	<1%

81	Jae-Won Choi, Yumi Cha, Jeoung-Yun Kim. "Change in the tropical cycl... Crossref	<1%
82	Chun-Sil Jin, Chang-Hoi Ho, Joo-Hong Kim, Dong-Kyou Lee, Dong-Hyun... Crossref	<1%
83	Haikun Zhao, Xingyi Duan, G. B. Raga, Philip J. Klotzbach. "Changes in ... Crossref	<1%
84	JAE-WON CHOI, YUMI CHA, RIYU LU. "The weakening of autumn droug... Crossref	<1%
85	Li Tao, Yufeng Lan. "Inter-decadal change of the inter-annual relations... Crossref	<1%
86	Liang Wu, Zhiping Wen, Ronghui Huang, Renguang Wu. "Possible Linka... Crossref	<1%
87	Ruifen Zhan, Yuqing Wang. "Weak Tropical Cyclones Dominate the Pol... Crossref	<1%
88	Zhanqiu Gong, Yusen Liu, Cheng Sun, Jing Zhang, Jianping Li, Chunmin... Crossref	<1%